# On finite element approximation of fluid-structure interactions with consideration of transition model

Petr Sváček

**Abstract** In this paper the numerical approximation of turbulent and laminar incompressible turbulent flow is considered. The mathematical model is either based on incompressible Navier-Stokes equations or on Reynolds averaged Navier-Stokes (RANS) equations enclosed by a turbulence model. The problem is discretized in space by the finite element method, the detailed description of the stabilization shall be given and several aspects of approximation of the turbulence/transition model shall be given. The numerical results of the finite element method shall be presented.

## 1 Introduction

Recently the mathematical modelling and numerical approximation play important role in the engineering practice in the civil, aerospace and mechanical engineering (see e.g. [3], [11]). Considering the fluid flow particularly the complicated phenomena such as turbulence can be treated using several approaches as direct numerical simulations (DNS), large eddy simulations (LES) or using the Reynolds averaged Navier-Stokes equations (RANS) approach, see e.g. [12]. In the technical practice the DNS/LES computations are usually not performed particularly due to their excessive requirements for both the memory and the CPU time. The Reynolds averaged Navier-Stokes equations (RANS) are recently being used, see [17]. The turbulence effects need to be taken into account even if the Reynolds number is relatively low. In this case also the transition from the laminar to the turbulent flow can influence the quality of the solution. There are three main possibilities how to include transition: the low-Reynolds modifications of the turbulence models or the $e^N$ method, which uses the local linear stability theory. Further, the empirical cor-

Petr Sváček
Czech Technical University in Prague, Faculty of Mechanical Engineering, Department of Technical Mathematics, Karlovo nám. 13, 121 35 Praha 2, Czech Republic, e-mail: Petr.Svacek@fs.cvut.cz

relations approach can be applied. These approaches can produce very good transition predictions (particularly for the flow over an airfoil), but their application for general CFD codes is usually complicated (due to several non-local operations). In order to include the transition model into aeroelastic simulations and avoid using the non-local operations, the transition model based on two transport equations for intermittency and the onset momentum-thickness Reynolds number were used, see [8], [14]. In the present paper we are concerned with the numerical simulation of the aeroelastic problem of 2D viscous incompressible flow past a moving airfoil. The main attention is paid to the description of the application of the $k-\omega$ turbulence model (see [17], [5]) together with the transition model included, see [8].

## 2 Mathematical description

In order to practically treat the numerical discretization on the moving computational domain $\Omega_t$, the Arbitrary Lagrangian-Eulerian (ALE) method is used, see [9], [10]. The ALE mapping $\mathscr{A} = \mathscr{A}(\xi,t) = \mathscr{A}_t(\xi)$ defined for all $t \in (0,T)$ and $\xi \in \Omega_0^{ref} = \Omega_0$ is assumed to be sufficiently smooth mapping from $\Omega_0$ onto $\Omega_t$. Further the domain velocity $\boldsymbol{w}_D$ is defined by $\boldsymbol{w}_D(x,t) = \frac{\partial \mathscr{A}}{\partial t}(\xi,t)$ for any $x = \mathscr{A}(\xi,t)$. The time derivative with respect to the reference configuration $\Omega_0^{ref}$ is called the ALE derivative, denoted as $D^{\mathscr{A}}/Dt$, see [15].

The mathematical formulation of the problem consists of the flow model, the structure model and the interface conditions. The fluid flow is described in the two-dimensional time dependent computational domain $\Omega_t \subset \mathbb{R}^2$ with the Lipschitz continuous boundary $\partial\Omega_t = \Gamma_D \cup \Gamma_O \cup \Gamma_{Wt}$. Here, $\Gamma_D$ denotes the inlet part of the computational domain, $\Gamma_O$ denotes the outlet part and $\Gamma_{Wt}$ denotes the surface of the airfoil at time $t$. The fluid motion in the domain $\Omega_t$ is modelled using the Navier-Stokes system of equations in $\Omega_t$ written in the ALE form ($i = 1,2$)

$$\frac{D^{\mathscr{A}} u_i}{Dt} + (\boldsymbol{u} - \boldsymbol{w}_D)\cdot\nabla u_i - \sum_{j=1}^{2} \frac{\partial}{\partial x_j}(2\nu S_{ij}) + \frac{\partial p}{\partial x_i} = 0, \quad \operatorname{div}\boldsymbol{u} = 0, \tag{1}$$

where $\boldsymbol{u} = (u_1,u_2)$ is the fluid velocity vector, $S_{ij} = \frac{1}{2}(\frac{\partial u_i}{\partial x_j} + \frac{\partial u_j}{\partial x_i})$ are the components of the symmetric part of the gradient of $\boldsymbol{u}$ denoted by $\boldsymbol{S} = \boldsymbol{S}(\boldsymbol{u})$, $p$ is the kinematic pressure (i.e., the pressure divided by the constant fluid density $\rho$), $\nu$ is the constant kinematic viscosity of the fluid (i.e., the viscosity divided by the density $\rho$). Let us note, that in the case of the Reynolds averaged Navier-Stokes equations the viscosity coefficient is replaced by $\nu_{\text{eff}} = \nu + \nu_T$, where $\nu_T$ is a turbulent viscosity (obtained by an additional model, see [17]).

The system (1) is equipped with boundary conditions

$$\begin{aligned} &\text{a) } \boldsymbol{u} = \boldsymbol{u}_D \quad \text{on } \Gamma_D, \qquad \text{b) } \quad \boldsymbol{u} = \boldsymbol{w}_D \quad \text{on } \Gamma_{Wt}, \\ &\text{c) } \quad -2\nu\boldsymbol{S}(\boldsymbol{u})\cdot\boldsymbol{n} + p\boldsymbol{n} + \tfrac{1}{2}(\boldsymbol{u}\cdot\boldsymbol{n})^{-}\boldsymbol{u} = 0 \quad \text{on } \Gamma_O, \end{aligned} \tag{2}$$

where $\alpha^- = \min(0,\alpha)$ denotes the negative part of the number $\alpha \in \mathbb{R}$ and $\boldsymbol{n} = (n_1, n_2)$ denotes the unit outward normal to $\partial\Omega_t$. Further, the system (1) is equipped with an initial condition $\boldsymbol{u}(x,0) = \boldsymbol{u}_0(x),\ x \in \Omega_0$.

The flow is interacting with a flexibly supported airfoil, which is allowed to be vertically displaced by $h$ (downwards positive) and rotated by the angle $\alpha$ (clockwise positive). Its motion is then described by the nonlinear equations of motion

$$\begin{aligned} m\ddot{h} + S_\alpha\,\ddot{\alpha}\cos\alpha - S_\alpha\dot{\alpha}^2\sin\alpha + k_h h &= -L(t), \\ S_\alpha\ddot{h}\cos\alpha + I_\alpha\ddot{\alpha} + k_\alpha\alpha &= M(t), \end{aligned} \tag{3}$$

where $m$ is the mass of the airfoil, $S_\alpha$ is the static moment around the elastic axis (EA), and $I_\alpha$ is the inertia moment around EA, see [15]. The parameters $k_h$ and $k_\alpha$ denote the bending and torsional spring stiffness coefficients, respectively. The aerodynamical lift force $L(t)$ and aerodynamical torsional moment $M(t)$ (clockwise positive) are given by

$$L = -l\int_{\Gamma_{Wt}}\sum_{j=1}^{2}\sigma_{2j}n_j\,dS,\quad M = l\int_{\Gamma_{Wt}}\sum_{i,j=1}^{2}\sigma_{ij}n_j r_i^{\mathrm{ort}}\,dS,\quad \sigma_{ij} = \rho\left[-p\delta_{ij} + 2\nu S_{ij}\right], \tag{4}$$

where $l$ denotes the depth of the airfoil section, $\delta_{ij}$ is the Kronecker's delta, $r_1^{\mathrm{ort}} = -(x_2 - x_2^{\mathrm{EA}})$, $r_2^{\mathrm{ort}} = x_1 - x_1^{\mathrm{EA}}$, and $x^{\mathrm{EA}} = (x_1^{\mathrm{EA}}, x_2^{\mathrm{EA}})$ is the position of EA of the airfoil at the time instant $t$.

## 3 Numerical approximation

For an arbitrary but fixed time instant $t$ we shall denote by $\boldsymbol{W}_t = \boldsymbol{H}^1(\Omega_t)$ the Sobolev space of vector square integrable functions together with their first derivatives and by $Q_t = L^2(\Omega_t)$ the Lebesgue space of square integrable functions. Further by $\boldsymbol{X}_t \subset \boldsymbol{H}^1(\Omega_t)$ the space of the test functions being zero on $\Gamma_D \cup \Gamma_{Wt}$ at the time instant $t$ shall be denoted. The weak formulation of the Navier-Stokes equations is obtained by multiplication of the first equation in (1) for $i = 1,2$ by $z_i$, the component of a test function $\boldsymbol{z} \in \boldsymbol{X}_t$, integration over the domain $\Omega_t$ and application of Green's theorem. Thus we get that $U = (\boldsymbol{u}, p) \in \boldsymbol{W}_t \times Q_t$ satisfies

$$\begin{aligned} \left(\frac{D^{\mathscr{A}}\boldsymbol{u}}{Dt}, \boldsymbol{z}\right) + \Big(2\nu\boldsymbol{S}(\boldsymbol{u}), \boldsymbol{S}(\boldsymbol{z})\Big) + c(\boldsymbol{u} - \boldsymbol{w}_D; \boldsymbol{u}, \boldsymbol{z}) - \Big(p, \nabla\cdot\boldsymbol{z}\Big) \\ + \frac{1}{2}\left((\nabla\cdot\boldsymbol{w}_D)\boldsymbol{z}, \boldsymbol{u}\right) = 0 \end{aligned}$$

for all $\boldsymbol{z} \in \boldsymbol{X}_t$ and $(\nabla\cdot\boldsymbol{u}, q) = 0$ for all $q \in Q_t$, where by $(\cdot,\cdot)$ the dot-product in $L^2(\Omega_t)$ is denoted, and

$$c(\overline{\boldsymbol{w}};\boldsymbol{u},\boldsymbol{z}) = \frac{1}{2}\Big((\overline{\boldsymbol{w}}\cdot\nabla)\boldsymbol{u},\boldsymbol{z}\Big) - \frac{1}{2}\Big((\overline{\boldsymbol{w}}\cdot\nabla)\boldsymbol{z},\boldsymbol{u}\Big) + \frac{1}{2}\int_{\Gamma_O}(\overline{\boldsymbol{w}}\cdot\boldsymbol{n})^{+}\boldsymbol{u}\cdot\boldsymbol{z}\,\mathrm{d}S.$$

In order to formulate the aerodynamical forces $L$ and $M$ also weakly, we shall use a function $\varphi \in H^1(\Omega_t)$ such that $\varphi(x,t) = 1$ for $x \in \Gamma_{Wt}$, and its compact support $\operatorname{supp}\varphi \subset \Omega_t \cup \Gamma_{Wt}$. Multiplying the first equation of (1) by the function $\boldsymbol{\Psi}^h = (0,\varphi)^T$, integrating over $\Omega_t$, applying Green's theorem to viscous and pressure terms, using the notation $\overline{\boldsymbol{w}} = \boldsymbol{u} - \boldsymbol{w}_D$, we get

$$\Big(\frac{D^{\mathscr{A}}\boldsymbol{u}}{Dt} + (\overline{\boldsymbol{w}}\cdot\nabla)\boldsymbol{u},\boldsymbol{\Psi}^h\Big) + \Big(2\nu\boldsymbol{S}(\boldsymbol{u}),\boldsymbol{S}(\boldsymbol{\Psi}^h)\Big) - \Big(p,\nabla\cdot\boldsymbol{\Psi}^h\Big) = \frac{1}{\rho}\int\limits_{\Gamma_{Wt}}\sigma_{ij}n_j\Psi_i^h\,\mathrm{d}S$$

Thus with the aid of (4) and having $\boldsymbol{\Psi}^h = (\Psi_1^h,\Psi_2^h) \in \boldsymbol{W}_t$ equal to $(0,1)^T$ on $\Gamma_{Wt}$, we get the weak form of the aerodynamical lift force $L$:

$$L = -\rho l\int_{\Omega_t}\frac{D^{\mathscr{A}}\boldsymbol{u}}{Dt}\cdot\boldsymbol{\Psi}^h + ((\overline{\boldsymbol{w}}\cdot\nabla)\,\boldsymbol{u})\cdot\boldsymbol{\Psi}^h - p(\nabla\cdot\boldsymbol{\Psi}^h) + 2\nu\,\boldsymbol{S}(\boldsymbol{u}) : \boldsymbol{S}(\boldsymbol{\Psi}^h)\,\mathrm{d}x. \quad (5)$$

Similarly using the vector-valued function $\boldsymbol{\Psi}^\alpha = (\Psi_1^\alpha,\Psi_2^\alpha) = \varphi\,(r_1^{\mathrm{ort}},r_2^{\mathrm{ort}})^T$ we get

$$M = \rho l\int\limits_{\Omega_t}\frac{D^{\mathscr{A}}\boldsymbol{u}}{Dt}\cdot\boldsymbol{\Psi}^\alpha + ((\overline{\boldsymbol{w}}\cdot\nabla)\,\boldsymbol{u})\cdot\boldsymbol{\Psi}^\alpha - p(\nabla\cdot\boldsymbol{\Psi}^\alpha) + 2\nu\,\boldsymbol{S}(\boldsymbol{u}) : \boldsymbol{S}(\boldsymbol{\Psi}^\alpha)\,\mathrm{d}x. \quad (6)$$

In order to discretize the problem in time the equidistant partition $t_k = k\Delta t$ of the time interval $I$ is considered with a time step $\Delta t > 0$. We denote the approximations $\boldsymbol{u}^k \approx \boldsymbol{u}(\cdot,t_k)$ and $p^k \approx p(\cdot,t_k)$. Moreover we approximate the domain velocity $\boldsymbol{w}_D$ at time level $t_k$ by $\boldsymbol{w}_D^k$ and focus on the description of the discretization at an arbitrary fixed time instant $t = t_{n+1}$. For the sake of simplicity we shall omit the subscripts $t$ or $t_{n+1}$ in what follows. We shall consider all the function spaces $\boldsymbol{X},\boldsymbol{W},Q$ defined for the time instant $t = t_{n+1}$ on the domain $\Omega := \Omega_{t_{n+1}}$. Then the ALE time derivative in the weak formulation of (1) is approximated at the time $t = t_{n+1}$ by the second order backward difference formula, i.e.,

$$\frac{D^{\mathscr{A}}\boldsymbol{u}}{Dt}|_{t=t_{n+1}} \approx \frac{3\boldsymbol{u}^{n+1} - 4\tilde{\boldsymbol{u}}^n + \tilde{\boldsymbol{u}}^{n-1}}{2\Delta t},$$

where by $\tilde{\boldsymbol{u}}^i = \boldsymbol{u}^i \circ \mathscr{A}_{t_i} \circ \mathscr{A}_{t_{n+1}}^{-1}$ the transformation of $\boldsymbol{u}^i$ from $\Omega_{t_i}$ on $\Omega$ for $i = n-1$ and $i = n$ is denoted.

In order to spatially discretize the problem (1) by the finite element method, the spaces $\boldsymbol{X},\boldsymbol{W}$ and $Q$ are approximated by finite element subspaces $\boldsymbol{X}_\Delta,\boldsymbol{W}_\Delta$ and $Q_\Delta$, respectively. The Taylor-Hood family of finite element spaces defined over a triangulation $\mathscr{T}_\Delta$ of the computational domain $\Omega = \Omega_{t_{n+1}}$ is used, i.e., the continuous piecewise quadratic velocities and the continuous piecewise linear pressures are used. Moreover for the involved high Reynolds numbers the fully stabilized scheme is used, which consists of streamline-upwind/Petrov-Galerkin (SUPG) and pressure-

stabilizing/Petrov-Galerkin (PSPG) stabilization combined with the div-div stabilization, see [4]. For $U,V,U^* \in \boldsymbol{W}_\Delta \times Q_\Delta$, $U=(\boldsymbol{u},p)$, $V=(\boldsymbol{z},q)$, $U^*=(\boldsymbol{u}^*,p)$ we define

$$\begin{aligned} a(U^*;U,V) &= \frac{3}{2\Delta t}\Big(\boldsymbol{u},\boldsymbol{z}\Big) + c(\boldsymbol{u}^* - \boldsymbol{w}_D^{n+1};\boldsymbol{u},\boldsymbol{z}) + \Big(2\nu\boldsymbol{S}(\boldsymbol{u}),\boldsymbol{S}(\boldsymbol{z})\Big) \\ &\quad + (\nabla\cdot\boldsymbol{u},q) - \Big(p,\nabla\cdot\boldsymbol{z}\Big) + \frac{1}{2}\Big((\nabla\cdot\boldsymbol{w}_D^{n+1})\,\boldsymbol{u},\boldsymbol{z}\Big), \\ L(V) &= \frac{1}{2\Delta t}\left(4\tilde{\boldsymbol{u}}^n - \tilde{\boldsymbol{u}}^{n-1},\boldsymbol{z}\right), \end{aligned}$$

and the terms $\mathscr{L}$ and $\mathscr{F}$ are the SUPG/PSPG terms defined by

$$\begin{aligned} &\mathscr{L}(U^*;U,V) \\ &\quad = \sum_{K\in\mathscr{T}_\Delta} \delta_K\Big(\frac{3\boldsymbol{u}}{2\Delta t} - \nu\triangle\boldsymbol{u} + \left(\overline{\boldsymbol{w}}^{n+1}\cdot\nabla\right)\boldsymbol{u} + \nabla p, \left(\overline{\boldsymbol{w}}^{n+1}\cdot\nabla\right)\boldsymbol{z} + \nabla q\Big)_K, \\ &\mathscr{F}(V) = \sum_{K\in\mathscr{T}_\Delta} \delta_K\Big(\frac{1}{2\Delta t}(4\tilde{\boldsymbol{u}}^n - \tilde{\boldsymbol{u}}^{n-1}), \left(\overline{\boldsymbol{w}}^{n+1}\cdot\nabla\right)\boldsymbol{z} + \nabla q\Big)_K, \end{aligned} \tag{7}$$

where the function $\overline{\boldsymbol{w}}^{n+1} = \boldsymbol{u}^* - \boldsymbol{w}_D^{n+1}$ stands for the transport velocity. Here, the constant viscosity assumption was used to simplify the viscous term to $\nu\triangle\boldsymbol{u}$. In the case of variable viscosity $\nu_{eff}$ either the viscous term needs to be modified or the elementwise constant viscosity $\nu_T$ is used.

**Problem 1 (Stabilized problem).** The stabilized discrete problem reads: Find $U = (\boldsymbol{u}_\Delta^{n+1}, p_\Delta^{n+1}) \in \boldsymbol{W}_\Delta \times Q_\Delta$ such that $\boldsymbol{u}_\Delta^{n+1}$ satisfies approximately the Dirichlet boundary conditions (2,a,b) and

$$a(U;U,V) + \mathscr{L}(U;U,V) + \sum_{K\in\mathscr{T}_\Delta} \tau_K(\nabla\cdot\boldsymbol{u},\nabla\cdot\boldsymbol{z})_K = L(V) + \mathscr{F}(V) \tag{8}$$

holds for all $V=(\boldsymbol{z},q) \in \boldsymbol{X}_\Delta \times Q_\Delta$, where the stabilizing parameters $\tau_K$ and $\delta_K$ for the Taylor-Hood family of finite elements are set to $\tau_K = \max_{x\in\Omega} \|\boldsymbol{u}^n(x)\|_2$ and $\delta_K = h_K^2/\tau_K$. This corresponds to the optimal choice in [4], particularly in the case if $\max_{x\in\Omega} \|\boldsymbol{u}^n(x)\|_2 \approx 1$.

The non-linear problem is then solved using the Oseen linearization process, where the solution of each of the linear problems is performed using an efficient direct solver, see [2].

## 4 Turbulent flow

For modelling of the turbulent flow with the transition the Menter's SST $k-\omega$ turbulence model, see [7] is used, with the $\gamma - \overline{Re}_{\theta t}$ transition model introduced by [8].

The viscosity coefficient $\nu$ in the equation (1) is replaced by the effective viscosity $\nu_{\text{eff}} = \nu + \nu_T$, and the turbulent viscosity $\nu_T$ is modelled using the turbulent kinetic energy $k = k(x,t)$ and the turbulent specific dissipation rate $\omega = \omega(x,t)$ satisfying for any $t \in (0,T)$ in $\Omega_t$ equations

$$\begin{aligned} \frac{D^{\mathscr{A}} k}{Dt} + ((\boldsymbol{u} - \boldsymbol{w}_D)\cdot\nabla)k &= \gamma_{\text{eff}} P_k - \beta^* \omega k \overline{\gamma_{\text{eff}}} + \nabla\cdot(\varepsilon_k \nabla k), \\ \frac{D^{\mathscr{A}} \omega}{Dt} + ((\boldsymbol{u} - \boldsymbol{w}_D)\cdot\nabla)\omega &= P_\omega - \beta\omega^2 + \nabla\cdot(\varepsilon_\omega \nabla\omega) + C_D, \end{aligned} \tag{9}$$

where $\varepsilon_k = \nu + \sigma_k \nu_T$, $\varepsilon_\omega = \nu + \sigma_\omega \nu_T$ and the source terms $P_k$, $P_\omega$ and $C_D$ are defined by

$$P_k = \nu_T S,\ S = \boldsymbol{S}(\boldsymbol{u}) : \boldsymbol{S}(\boldsymbol{u}),\ P_\omega = \frac{\alpha_\omega \omega}{k} P_k,\ C_D = 2(1-F_1)\frac{\sigma_D}{\omega}(\nabla k \cdot \nabla\omega)^+$$

and the turbulent viscosity is then given by

$$\nu_T = \min\Big(\frac{k}{\max(\omega, SF_2/a_1)}, \frac{0.6k}{\sqrt{3}S}\Big). \tag{10}$$

The closure coefficients $\beta$, $\beta^*$, $\sigma_k$, $\sigma_\omega$, $\alpha_\omega$ are chosen according to [7], i.e., $a_1 = 0.3$, $\kappa = 0.41$, $\beta^* = 0.09$, $\sigma_D = 0.5$ and the coefficients $\sigma_k$, $\sigma_\omega$, $\beta$ and $\alpha_\omega$ are calculated using the blending function $F_1$ as $\phi = F_1\phi_1 + (1-F_1)\phi_2$, where $\sigma_{k1} = 0.85$, $\sigma_{\omega 1} = 0.65$, $\beta_1 = 0.075$, $\sigma_{k2} = 1$, $\sigma_{\omega 2} = 0.856$, $\beta_2 = 0.0828$ and $\alpha_\omega = \beta/\beta^* - \sigma_\omega \kappa^2/\sqrt{\beta^*}$. For the sake of brevity, the blending functions $F_1$, $F_2$ are not specified here, see e.g., [7]. In order to capture the transition, the modification of the SST model in the production and the destruction terms of (9) is used, using the effective intermittency $\gamma_{\text{eff}}$, $\overline{\gamma}_{\text{eff}} = \max(\min(\gamma_{\text{eff}}, 1), 0.1)$.

The effective intermittency is then modelled using the equation for the intermittency coefficient $\gamma$ written in the ALE form

$$\frac{D^{\mathscr{A}} \gamma}{Dt} + ((\boldsymbol{u} - \boldsymbol{w}_D)\cdot\nabla)\gamma = P_\gamma - E_\gamma + \nabla\cdot((\nu + \nu_T/\sigma_f)\nabla\gamma), \tag{11}$$

where $P_\gamma$ and $E_\gamma$ are the transition source and destruction terms given by $P_\gamma = F_{\text{length}} c_{a1} S \sqrt{\gamma F_{\text{onset}}}(1 - c_{e1}\gamma)$, and $E_\gamma = c_{a2}\Omega\gamma F_{\text{turb}}(c_{e2}\gamma - 1)$, where $S$ and $\Omega$ are the strain rate and vorticity magnitudes, respectively. Further, $F_{\text{onset}} = (F_{\text{onset2}} - F_{\text{onset3}})^+$, $F_{\text{onset1}} = \frac{Re_V}{2.193 Re_{\theta c}}$, $Re_V = \frac{y^2 S}{\nu}$, $R_T = \frac{k}{\nu\omega}$, $F_{\text{turb}} = e^{-(R_T/4)^4}$, $y$ denotes the wall distance, and $Re_{\theta t}$ is the transition Reynolds number and

$$F_{\text{onset2}} = \min\left(\max\left(F_{\text{onset1}}, F_{\text{onset1}}^4\right), 2\right), \qquad F_{\text{onset3}} = \max\left(1 - \left(\frac{R_T}{2.5}\right)^3, 0\right).$$

The following constants for the intermittency equation were used $c_{e1} = 1$, $c_{a1} = 2$, $c_{e2} = 50$, $c_{a2} = 0.06$, $\sigma_f = 1$. Further, $Re_{\theta c}$ is the critical Reynolds number given by an empirical correlation, and another empirical correlation is used for the function

$F_{\text{length}}$, which controls the length of the transition region. The correlations are based on newly defined transported unknown $\overline{Re}_{\theta t}$ governed by the equation written in the ALE form

$$\frac{D^{\mathscr{A}}\overline{Re}_{\theta t}}{Dt} + ((\boldsymbol{u}-\boldsymbol{w}_D)\cdot\nabla)\overline{Re}_{\theta t} = P_{\theta t} + \nabla\cdot(\sigma_{\theta t}\nu_{\text{eff}}\nabla\overline{Re}_{\theta t}), \tag{12}$$

where the source term $P_{\theta t} = c_{\theta t}\frac{\rho}{t_\infty}\left(Re_{\theta t} - \overline{Re}_{\theta t}\right)(1-F_{\theta t})$, where $c_{\theta t} = 0.03$, $\sigma_{\theta t} = 2$, $t_\infty = 500\nu/U^2$ is the time scale, $U$ is the magnitude of velocity $U = \|\boldsymbol{u}\|_2$ and the blending function $F_{\theta t}$ is defined as

$$F_{\theta t} = \min\left(1, \max\left(F_{\text{wake}}e^{-(y/\delta)^4}, 1-\left(\frac{\gamma - 1/c_{e2}}{1-1/c_{e2}}\right)\right)\right),$$

with $\delta = \frac{375\Omega y}{U}\theta$, $\theta = \frac{\overline{Re}_{\theta t}\nu}{U}$, $F_{\text{wake}} = e^{-(Re_\omega/10^5)^2}$, and $Re_\omega = \frac{\omega y^2}{\nu}$. The right hand side includes the Reynolds number $Re_{\theta t} = \theta_t\nu/U$ given by an empirical correlation specified later.

Here, we present the empirical correlations published in [6]. First, the length of the transition is controlled by

$$F_{\text{length}} = \begin{cases} 39.82 - 0.119\overline{Re}_{\theta t} - \frac{1.33}{10^4}\overline{Re}_{\theta t}^2 & \text{for } \overline{Re}_{\theta t} < 400, \\ 263.4 - 1.24\overline{Re}_{\theta t} + \frac{1.95}{10^3}\overline{Re}_{\theta t}^2 - \frac{1.02}{10^6}\overline{Re}_{\theta t}^3 & \text{for } 400 \le \overline{Re}_{\theta t} < 596, \\ 0.5 - \frac{3}{10^4}\left(\overline{Re}_{\theta t} - 596\right) & \text{for } 596 \le \overline{Re}_{\theta t} < 1200, \\ 0.3188, & \text{for } 1200 \le \overline{Re}_{\theta t}. \end{cases}$$

The transitional onset momentum thickness Reynolds number $Re_{\theta t}$ is correlated to pressure gradient $\lambda_\theta$ and to turbulence intensity $Tu$ defined by

$$\lambda_\theta = \frac{\theta_t^2}{\nu}\frac{\partial U}{\partial \boldsymbol{u}}, \qquad Tu = 100\frac{\sqrt{2k/3}}{U},$$

where $\frac{\partial U}{\partial \boldsymbol{u}}$ is the acceleration of the flow velocity in the streamwise direction. The correlation for $Re_{\theta t}$ is given by

$$Re_{\theta t} = \begin{cases} \left(1173.51 - 589.428Tu + \frac{0.2196}{Tu^2}\right)F(\lambda_\theta), & \text{for } Tu \le 1.3, \\ 331.5\left(Tu - 0.5658\right)^{-0.671}F(\lambda_\theta), & \text{for } Tu > 1.3, \end{cases}$$

where the function $F(\lambda_\theta)$ reads

$$F(\lambda_\theta) = \begin{cases} 1 - \left(-12.986\lambda_\theta - 123.66\lambda_\theta^2 - 405.689\lambda_\theta^3\right)e^{-(2Tu/3)^{3/2}}, & \text{for } \lambda_\theta \le 0, \\ 1 + 0.275\left(1 - e^{-35\lambda_\theta}\right)e^{-2Tu}, & \text{for } \lambda_\theta > 0. \end{cases}$$

Last, the correlation for the critical Reynolds number is given by the relation

$$Re_{\theta c} = \begin{cases} \frac{101.21}{10^2}\overline{Re}_{\theta t} - 3.96 - 8.68\,\frac{\overline{Re}^2_{\theta t}}{10^4} + 6.97\,\frac{\overline{Re}^3_{\theta t}}{10^7} - 1.74\frac{\overline{Re}^4_{\theta t}}{10^{10}} & \frac{\overline{Re}_{\theta t}}{1870} \le 1, \\ \overline{Re}_{\theta t} - 593.11 - 0.482(\overline{Re}_{\theta t} - 1870) & \frac{\overline{Re}_{\theta t}}{1870} > 1. \end{cases}$$

The effective intermittency is then taken as $\gamma_{\text{eff}} = \max(\gamma, \gamma_{sep})$ where

$$\gamma_{sep} = F_{\theta t} \min\left(2{,}2\left(\frac{Re_V}{3.235 Re_{\theta c}} - 1\right)^+\right) e^{-(\frac{R_T}{20})^4}.$$

The equations (11) and (12) are equipped with the Dirichlet boundary conditions at the inlet ($\gamma = 1$, $\overline{Re}_{\theta t}$ obtained by the previously specified correlation for $Re_{\theta t}$) and Neummann boundary conditions at the outlet and on the airfoil surface ($\Gamma_O \cup \Gamma_{Wt}$). The initial values are set to be equal to the inlet boundary condition. The turbulence and transition models are linearized, time discretized, and approximated by the SUPG stabilized finite element method. The resulting system of linear equations is solved numerically using the direct solver.

## 5 Numerical results

The aeroelastic response of a typical airfoil section to both the light and heavy gusts was studied. The input parameters were chosen according to [1] and the results were also compared with the numerical results of the author [16], where no turbulent-laminar flow transition was considered. The airfoil shape was given by a conformal transformation and two shapes of the airfoil (A1 and A2) were considered, see [16]. The airfoil parameters were as follows: the mass $m = 2 \times 10^{-4}$ kg the inertia and static moments $I_\alpha = 1.2 \times 10^{-7}$ kg m$^2$ and $S_\alpha = 2 \times 10^{-6}$ kg m, respectively, the chord $c = 0.1$ m, the elastic axis was located at 30 % of the chord, the center of gravity was at 40 % of the chord, and the depth of the airfoil section was $l = 0.03$ m. The stiffness coefficients of the springs were $k_h = 26$ N/m, $k_\alpha = 0.29$ N m/rad for the airfoil A1 and $k_h = 42.5$ N/m, $k_\alpha = 0.68$ N m/rad for the airfoil A2. The air density was $\rho = 1.225\,\text{kg m}^{-3}$ and the air kinematic viscosity was $\nu = 1.453 \times 10^{-5}\,\text{m}^2/\text{s}$. The inlet turbulence intensity was 1% ($k = 1.5 \times 10^{-4} U_\infty^2$, $\omega = 10\,\text{s}^{-1}$ on $\Gamma_I$). The vertical gust of 1 $s$ duration was considered as a sudden perturbation of the aeroelastic system for $t \in [t_0, t_0 + 1]$ $V_g(t) = \frac{V_G}{2}\,(1 + \cos(\pi(t - t_0)))$, where $V_G = 1.5\,\text{m s}^{-1}$ and $V_G = 5\,\text{m s}^{-1}$ were considered for the light and heavy gusts, respectively. The numerical simulation of the aeroelastic response of the airfoil started from the zero initial conditions and $V_G = 0$ and the constant far field stream velocity $U_\infty = 15\text{m s}^{-1}$. The time step was chosen equal to $\Delta t = 6.6667 \times 10^{-5}$ s.

The aeroelastic airfoil responses $h(t)$ and $\alpha(t)$ for the light gust are shown in Figs. 1, 2, and compared to the laminar (no turbulence, $\nu_T \equiv 0$) and $k - \omega$ turbulent models. The computations were performed up to the time $t \ge 1$ s, when the responses to the gust nearly faded out. During the beginning phase of the simulation $t \ge -0.05$ s the airfoil is fixed in the horizontal position, then the airfoil is released

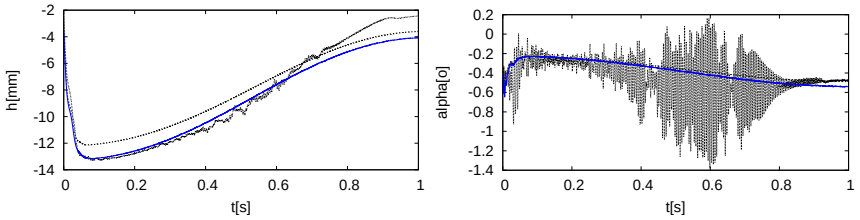


**Fig. 1** Aeroelastic response to the light gust, airfoil A1: Comparison of the aeroelastic response computed by laminar (solid line), turbulent (dashed) and transitional (dotted) models.

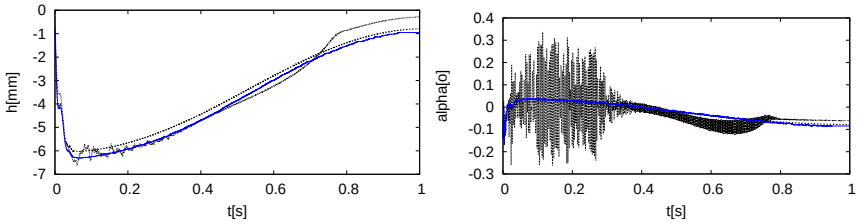


**Fig. 2** Aeroelastic response to the light gust, airfoil A2: Comparison of the aeroelastic response computed by laminar (solid line), turbulent (dashed) and transitional (dotted) models.

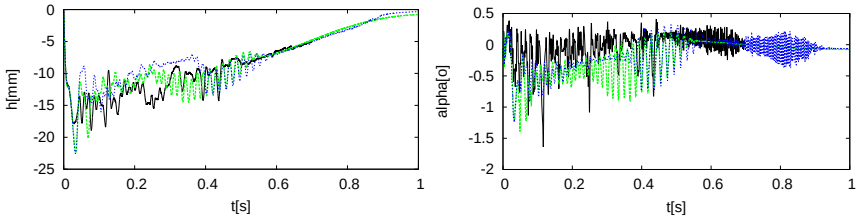


**Fig. 3** Aeroelastic response to the heavy gust, airfoil A2: Comparison of the aeroelastic response computed by laminar (solid line), turbulent (dashed) and transitional (dotted) models.

and moves to a static position. Afterwards at the time instant $t = 0\,\mathrm{s}$ the sudden vertical gust starts to load the airfoil. Similarly, the numerically simulated airfoil responses $h(t)$ and $\alpha(t)$ for the heavy gust ($V_G = 5\,\mathrm{m\,s^{-1}}$) are shown in Fig. 3. The results for the transitional flow model are close to the simulations using the turbulence model. A too noisy response for the rotation angle $\alpha(t)$ resulted from the laminar model both for the light and heavy gust. Figure 4 shows the airflow velocity patterns for the laminar, turbulent and transitional flow models, respectively, at the time $t_0$ just before the gust starts. Many small eddies are shed in the airfoil wake for the laminar flow model. Practically no eddies are visible in a wider wake for turbulent flow model and much narrow wake results from the transitional model, where a laminar flow exists on the large portion of the profile surface. It is supported by the turbulent kinetic energy pattern around the airfoil shown in Fig. 5, where the most of the turbulent kinetic energy is in a far wake and almost zero turbulent kinetic energy is at the airfoil surface.

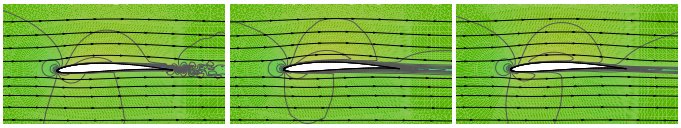

**Fig. 4** Comparison of velocity flow patterns for the laminar (left), turbulent (middle) and transitional (right) models just before the gust starts, airfoil A1.

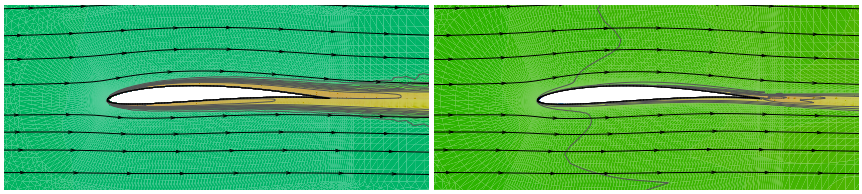

**Fig. 5** Comparison of the turbulent kinetic energy $k$ distribution for the turbulent (left) and transitional (right) models just before the gust starts, airfoil A1.

## 6 Conclusion

The present paper describes the solution of FSI problem of flow induced vibrations with the consideration of a sudden gust. The problem is discretized in space using the finite element method. The main attention is paid to the description of the transition model, originally proposed by [8], but the necessary theoretical correlations was not specified there. These were later specified also by different authors as [13], and also by [6]. In this paper, we focus on the detailed presentation of the transitional model, which was implemented into the in-house FE code and applied for solution of FSI. The numerical results were compared with the relevant results.

**Acknowledgements** This work was supported by the grant No. P101/12/1271 of the Czech Science Foundation.

## References

1. M. Berci, S. Mascetti, A. Incognito, P. H. Gaskell, and V. V. Toropov. Gust response of a typical section via CFD and analytical solutions. In J. C. F. Pereira and A. Sequeira, editors, *ECCOMAS CFD 2010, V. European Conference on Computational Fluid Dynamics*, page 10 pp., 2010.
2. T. A. Davis and I. S. Duff. A combined unifrontal/multifrontal method for unsymmetric sparse matrices. *ACM Transactions on Mathematical Software*, 25:1–19, 1999.
3. Earl H. Dowell and Robert N. Clark. *A modern course in aeroelasticity*. Solid mechanics and its applications. Kluwer Academic Publishers, Dordrecht, Boston, 2004.
4. T. Gelhard, G. Lube, M. A. Olshanskii, and J.-H. Starcke. Stabilized finite element schemes with LBB-stable elements for incompressible flows. *Journal of Computational and Applied Mathematics*, 177:243–267, 2005.

5. J. C. Kok. Resolving the dependence on free-stream values for the k-omega turbulence model. Technical report, National Aerospace Laboratory NLR, 1999.
6. Robin B. Langtry and F R Menter. Correlation-based transition modeling for unstructured parallelized computational fluid dynamics codes. *AIAA JOURNAL*, 47(12):2894–2906, 2009.
7. F. R. Menter. Two-equations eddy-viscosity turbulence models for engineering applications. *AIAA Journal*, 32(8):1598–1605, 1994.
8. FR Menter, R Langtry, and S Völker. Transition modelling for general purpose CFD codes. *Flow, Turbulence and Combustion*, 77(1-4):277–303, 2006.
9. F. Nobile. *Numerical approximation of fluid-structure interaction problems with application to haemodynamics*. PhD thesis, Ecole Polytechnique Federale de Lausanne, 2001.
10. T. Nomura and T. J. R. Hughes. An arbitrary Lagrangian-Eulerian finite element method for interaction of fluid and a rigid body. *Computer Methods in Applied Mechanics and Engineering*, 95:115–138, 1992.
11. M.P. Paidoussis. *Fluid-Structure Interactions. Slender structures and axial flow*. Academic Press, Elsevier, 2013. 2nd Edition.
12. S. B. Pope. *Turbulent Flows*. Cambridge University Press, Cambridge, 2000.
13. Keerati Suluksna and Ekachai Juntasaro. Assessment of intermittency transport equations for modeling transition in boundary layers subjected to freestream turbulence. *International Journal of Heat and Fluid Flow*, 29(1):48 – 61, 2008.
14. Y.B. Suzen, P.G. Huang, L. S. Hultgren, and D. E. Ashpis. Predictions of separated and transitional boundary layers under low-pressure turbine airfoil conditions using an intermittency transport equation. *Journal of turbomachinery*, 125(3):455–464, 2003.
15. P. Sváček, M. Feistauer, and J. Horáček. Numerical simulation of flow induced airfoil vibrations with large amplitudes. *Journal of Fluids and Structures*, 23(3):391–411, 2007.
16. Petr Sváček and Jaromír Horáček. On mathematical modeling of fluid–structure interactions with nonlinear effects: Finite element approximations of gust response. *Journal of Computational and Applied Mathematics*, 273(0):394 – 403, 2015.
17. D. C. Wilcox. *Turbulence Modeling for CFD*. DCW Industries, 1993.